

AN ABSTRACT OF THE THESIS OF

Hemendra G. Godbole for the degree of Master of Science in Electrical and Computer Engineering presented on January 27, 1989.

Title: An Investigation of Bulk Stacking Faults in Silicon Using Photocapacitance Transient Spectroscopy.

Abstract approved: \_\_\_\_\_

**Redacted for Privacy**

 Professor Leonard Forbes

Imperfections in semiconductor materials constitute a rich area for research. The importance of the characterization of these imperfections cannot be understated. Junction spectroscopic techniques provide a unique tool for the study of these imperfections. The test specimens could consist of Schottky barrier, p-n junctions, or MOS structures.

Using Schottky barrier diode structures on silicon, and stimulating the bulk stacking faults with incident photon energies, leads to a characterization technique of the defects. This technique is termed as the Photocapacitance Transient Spectroscopy, and is described in detail. The measurements show a dominant energy level at  $E_c - E_t = 0.45 + 0.05$  eV. due to oxygen induced stacking faults. The results obtained have been compared to those obtained by a different technique (termed the "Deep Level Transient Spectroscopy"). These results are shown to exhibit a high degree of correlation.

An Investigation of Bulk Stacking Faults in Silicon  
Using Photocapacitance Transient Spectroscopy

by

Hemendra G. Godbole

A THESIS

submitted to

Oregon State University

in partial fulfillment of  
the requirements for the  
degree of

Master of Science

Completed January 27, 1989

Commencement June 1989

APPROVED:

Redacted for Privacy

Professor of Electrical and Computer Engineering in charge of  
major

Redacted for Privacy

Head of department of Electrical and Computer Engineering

Redacted for Privacy

Dean of Graduate School

Date thesis is presented: January 27 , 1989

Typed by researcher for: Hemendra G. Godbole

#### ACKNOWLEDGEMENT

I express my sincere appreciation to Professor Len. Forbes for his guidance, and support during the investigation. I am grateful to Dr. Vijay Tripathi and Dr. Saife Kiaie for their timely reviews of the manuscript and helpful suggestions.

Also to be thanked are Mr. Tom Dobson for his help in generating the computer program, and Mr. Homayoon Haddad for his guidance and continued encouragement throughout the experimental phases of the work.

## TABLE OF CONTENTS

|  | Page |
|--|------|
| I INTRODUCTION .....   | 1    |
| II PHOTOCAPACITANCE TRANSIENT SPECTROSCOPY : THEORY...               | 5    |
| III FABRICATION AND CHARACTERIZATION OF<br>THE SCHOTTKY DIODES ..... | 15   |
| IV EXPERIMENTAL SETUP AND PROCEDURE .....                            | 23   |
| V RESULTS AND DISCUSSION .....                                       | 33   |
| VI REFERENCES .....  | 40   |
| APPENDICES   |      |
| A : MEASUREMENT ALGORITHM .....                                      | 41   |
| B : PARAMETRIC SETTINGS ON THE HP 4280A .....                        | 43   |
| C : PRECAUTIONS TO BE TAKEN DURING THE<br>MEASUREMENT .....          | 44   |

## LIST OF FIGURES

| Figure | Title  | Page |
|--------|--|------|
| 1      | Photoionisation cross section of Indium in Silicon as a function of photon energy<br>(b) Lucovsky model [5] using square well approximation, after A.G.Milnes [12] ..... | 3    |
| 2      | Kinetics of the processes in response to an optical stimulus, after R. Pierret et. al. [15] ...  | 9    |
| 3      | Arrhenius plot of emission rates for wafers used in the experiments, after L. Forbes et. al. [4] .....   | 10   |
| 4      | Cross-sectional view of the Schottky diodes used in the experiments .....  | 11   |
| 5      | Formation of the bulk stacking faults due to interstitial oxygen, after L. Forbes et. al. [4] ..   | 16   |
| 6      | Heat treatments used to generate the stacking faults, after L. Forbes et. al. [4] .....  | 17   |
| 7      | Schematic of the etching used during the fabrication of the Schottky diodes, after L. Forbes et. al. [4]   | 18   |
| 8      | Current v/s Voltage characteristic for a sample diode .....  | 20   |
| 9      | Capacitance v/s Voltage characteristic for a sample diode .....  | 21   |
| 10     | Capacitance DLTS results on a sample diode, after L. Forbes et. al. [4] .....  | 22   |
| 11     | Measured absorption coefficient for pure Ge, Si, GaAs, after S.M.Sze [11] .....  | 25   |
| 12     | A schematic of the experimental setup .....  | 28   |
| 13     | Capacitance v/s Time plot for a sample diode .....   | 34   |
| 14     | Log ( $\Delta C$ ) v/s time plot for a sample diode .....  | 35   |
| 15     | Optical Cross-section dependance on photon energy for a sample diode .....   | 38   |

LIST OF FIGURES (Continued)

| Figure | Title   | Page |
|--------|---|------|
| 16     | A comparision between DLTS and PCTS for<br>sample # 55B ..... | 39   |

# AN INVESTIGATION OF BULK STACKING FAULTS IN SILICON USING PHOTOCAPACITANCE TRANSIENT SPECTROSCOPY

## I. INTRODUCTION

Over a period of time now, different material characterization techniques have evolved that use semiconductor junctions as test devices. The issue of the accuracy and reliability of each technique is a sensitive one, and has undeniable commercial repercussions. The broadly used characterization techniques could be viewed to consist of three main classes: Capacitance transient spectroscopy, SEM charge collection microscopy, and Electroluminescence.

The technique investigated here belongs to the first category. This thesis shall review the theory that supports the technique, describe the measurement system in detail, and discuss the results to prove its utility in characterizing the imperfections in a large variety of cases.

Capacitance transient spectroscopy is a powerful form of a class of measurements which detect the current or capacitance response of a semiconductor junction to various external stimuli. These methods were first summarized by Sah et. al. [1] in 1970. The method used here is based on controlling the occupation of the imperfections in the depletion region in response to incident photons at different energies.



The emission or capture processes can be accurately monitored as a change in the reverse biased junction capacitance. Using the depletion region of the junction ensures isolation from free carriers in the semiconductor. Reviews which summarize developments in experimental techniques and applications have been summarized by Miller et. al. [6], Grimmeiss [7], Kimerling [8], Lang [9], and Chen and Milnes [10].

Photon stimulated emission processes have been summarized by White [2] and Bois et. al. [3]. Typically, the Photocapitance change is a slowly varying function of the incident photon energy, and fitting parameters are required to determine the threshold energy and Optical cross section.

The defects under investigation, were oxygen induced bulk stacking faults in Czochralski grown Silicon. These arise as precipitate induced microdefects, formed by the interstitial oxygen. The interstitial oxygen induces defects due to the thermal stresses it is subjected to. The formation and nature of this class of defects in CZ silicon have been discussed in detail by L.Forbes et. al. [4].

The characterization of the deep level impurities could encompass a number of parametric measurements. The most important of these are the energy position of these defects in the forbidden energy gap, and variation of the Optical cross section with the incident photon energy. The results obtained here are consistent with the Lucovsky

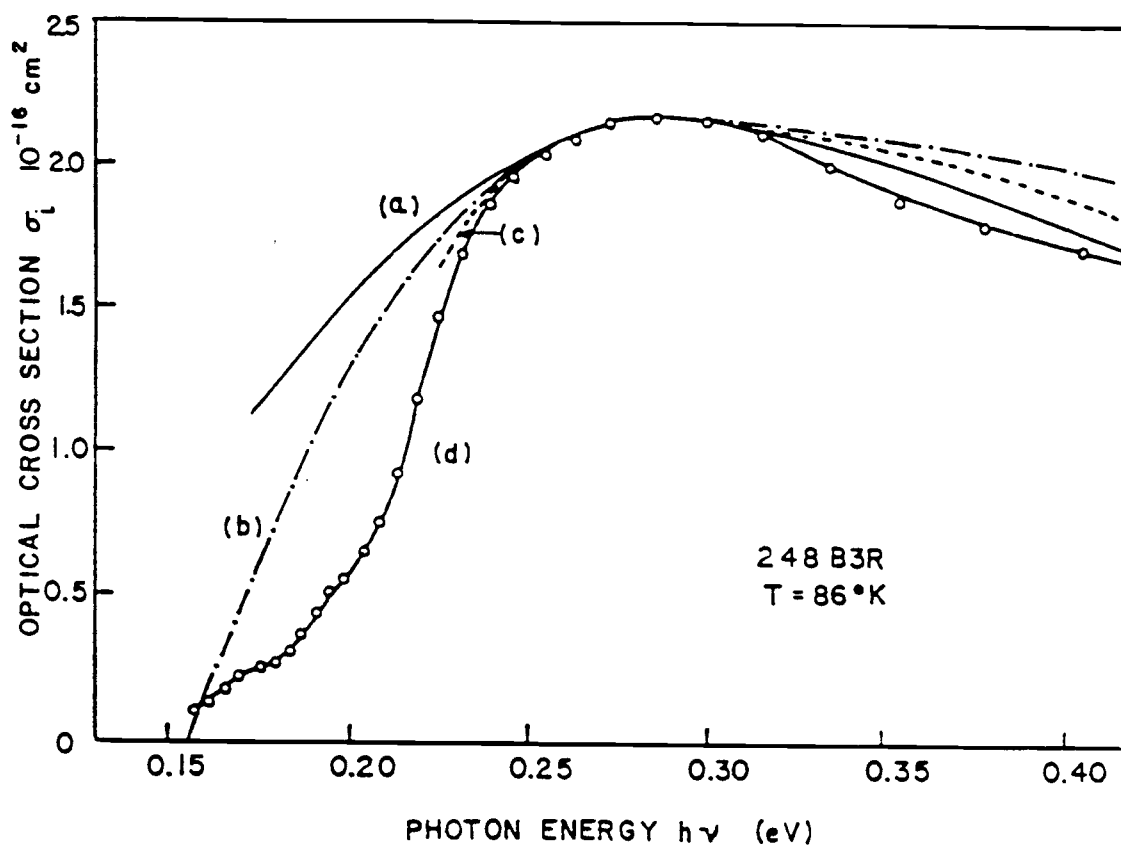


Figure 1) Photoionization cross section of Indium in Silicon as a function of photon energy  
 (b) Lucovsky model [5] using Square well approximation, after A.G. Milnes [12].

model [5], Fig. 1.

The test specimens used were Schottky diodes, consisting of aluminium evaporated on the bulk silicon. Contacts were bonded onto the metal and the substrate, and the diode mounted in an IC pad. The energy level predicted by the Photocapacitance transient measurements is in close agreement to that reported by DLTS measurements done on the same diodes. This further authenticates the observations, and suggests the use of this technique to investigate defects in other semiconductors as well.

## II. PHOTOCAPACITANCE TRANSIENT SPECTROSCOPY: THEORY.

A defect state may be defined as an electronic energy state introduced into the forbidden gap of a semiconductor as a consequence of a perturbation of the bonding structure of the host material. The disturbance could be caused by a lattice defect or an impurity. Electronic transitions at the defect site necessitate the classification of defects into "shallow states" and "deep states".

Shallow states are located near their related band edges (valence band for acceptors and conduction bands for donors) and the associated ionization energy can be approximately described by a modified hydrogenic model. These states typically relate to substitutional impurities which possess single excess (donor) or single deficient (acceptor) valence electron structure, relative to the atom replaced in the host material.

Deep states may be most simply classified as those which are positioned deeper than the corresponding hydrogenic states. This definition includes acceptors near the conduction band and donors near the valence band. The class of defects being studied here could be classified as "deep states".

"Capacitance transient spectroscopy" is a broad field of characterization techniques. The two most widely used techniques in this domain are the "Deep Level Transient Spectroscopy" (DLTS), and Photocapacitance transient

spectroscopy. Both of these deal with the time domain studies of the relaxation of a physical system following an abrupt disturbance.

By the artifice of employing semiconductor materials in the form of reverse biased p-n junction structures (or Schottky diodes), it is possible to carry out transient capacitance measurements. Such measurements are made in a region of the semiconductor that is essentially devoid of mobile carriers; this provides a convenient location for the observation of isolated electronic transitions.

There exists one principal limitation to these techniques: These are electrical measurements, implying thereby, that only electrically active centers can be observed. Consequently, if some defect or species of interest is uncharged or unipolar, or does not create an energy level in an accessible location (such as within the forbidden gap in a semiconductor material), it will not be observable.

Czochralski crystals contain oxygen concentrations of about  $1 \times 10^{18} / \text{cm}^3$ . These oxygen atoms are located interstitially and are not electrically active; however, during crystal growth or internal gettering cycles, these become significant. They can form precipitates ranging in size from 10 Å. to 1000 Å. These precipitates act as nuclei of secondary defects such as stacking faults or dislocation loops when subjected to different heat treatments during device processing. Electrical activity of stacking faults has been previously investigated by Kimerling et al. [13]

using a Charge Collection Scanning Electron Microscope (CCSEM) and theoretical calculations by Weigel et al. [14] shows only a minor charge redistribution around a stacking fault. From these studies, it has been concluded that the possibility of impurities being the cause of the observed electrical activity is non-existent. Instead, the stacking faults themselves are electrically active. Deep Level Transient Spectroscopy (DLTS) measurements have revealed a dominant energy level at  $E_C - E_T = 0.48$  eV. due to oxygen induced stacking faults. Low temperature, Photocapacitance transient measurements have been used here to further investigate the energy levels. The measurements were made on the same samples used for DLTS measurements to ensure a correlation of the observations.

The kinetics of the three state system can get highly complicated. For the understanding of the Photocapacitance transient measurements, however, a simple model is adequate ( Fig. 2 ) .

For the n-type sample, applying a negative potential at the metal electrode causes the Schottky diode to be reverse-biased. The depletion width extends entirely into the silicon, thereby uncovering the stacking faults at the surface. As pointed out before, these stacking faults are electrically active, and can be conceptualised to denote an energy level (or, a spread of energy levels) in the forbidden gap. This trap level is capable of generating transitions from the trap level to the conduction band.

At room temperature, any transitions induced within the bandgap due to the absorption of photons would be insignificant as compared to the transitions due to thermal absorption. As can be seen from the Arrhenius plot, Fig. 3, transitions due to phonon absorption is significantly reduced at lower temperatures. If the Schottky diode was subjected to a photonic bombardment at temperatures as low as 120 K., the concurrent transitions from the trap to the conduction band would be almost entirely due to photonic absorption.

The trapped electrons (at the energy level  $E_T$ ), when subjected to optical radiation within the bandgap, absorb energy, and can jump over to the conduction band. (Provided that the radiation  $h$  is greater than  $E_C - E_T$ ). This loss of trapped electrons results in a change in the density of trapped electrons; the change in density implies a change in the depletion width of the Schottky diode, which in turn results in a change in the capacitance of the diode. The small-signal capacitance of the junction is given by:

$$C = \frac{\epsilon A}{W} \quad (1)$$

where,  $A$  is the area of the junction,  $\epsilon$  is the dielectric constant, and  $W$  is the depletion width.

A small change in the capacitance is given by:

$$\frac{\Delta C}{C} = \frac{\Delta W}{W} \quad (\text{in magnitude}) \quad (2)$$

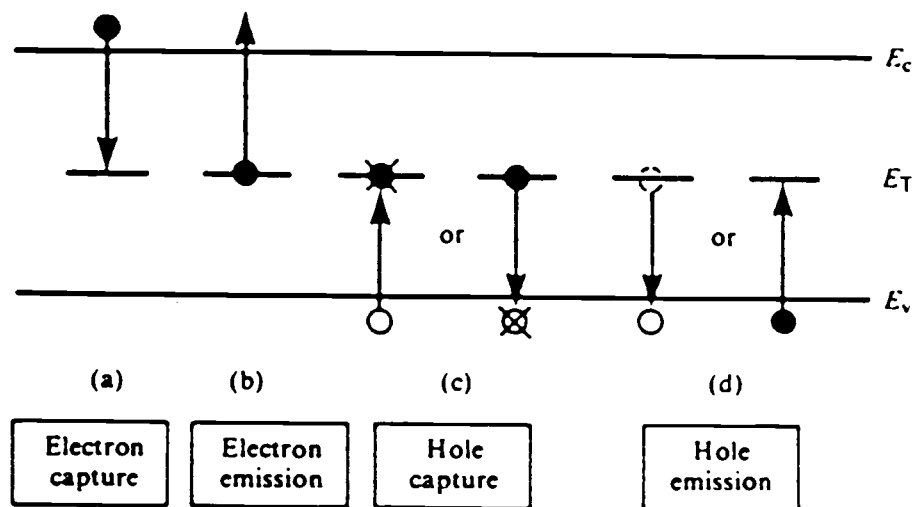


Figure 2) Kinetics of the processes in response to an optical stimulus, after R. Pierret et. al., [15].



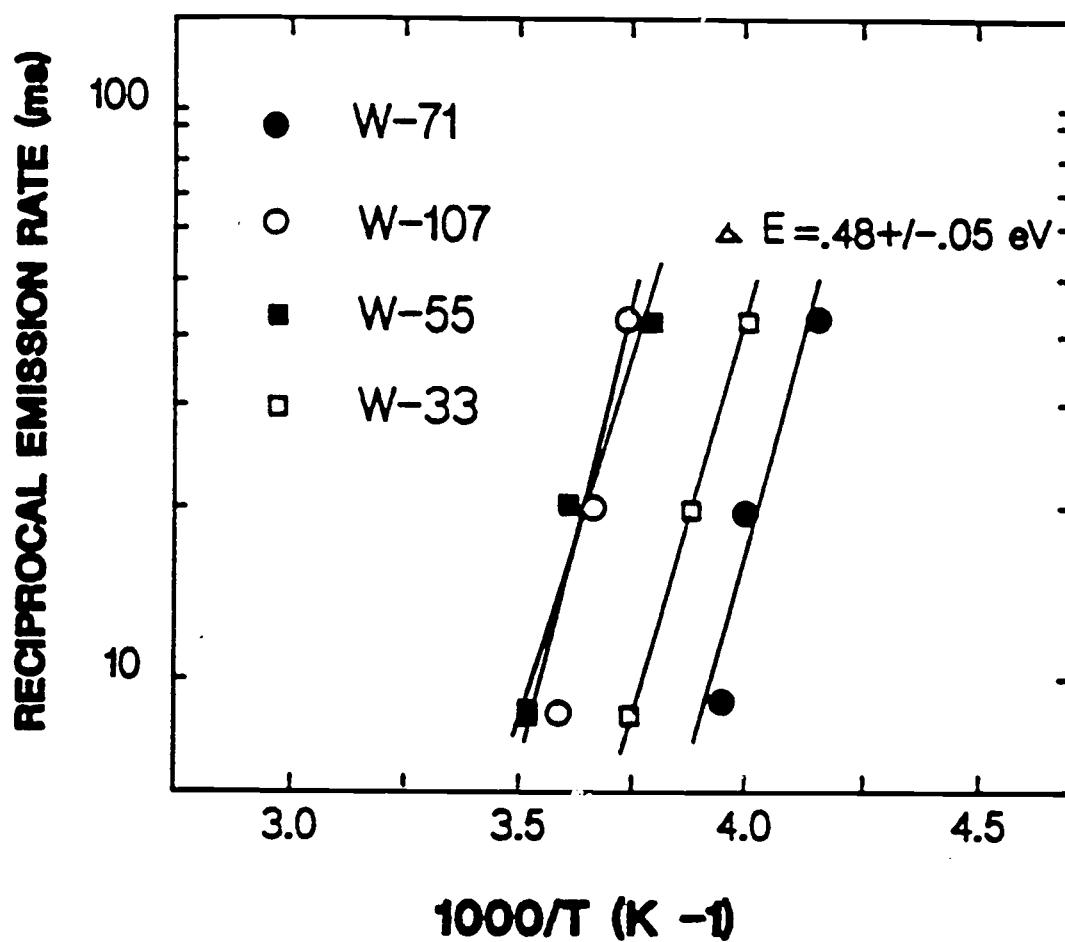


Figure 3) Arrhenius plot of emission rates for wafers used in the experiments, after L. Forbes et. al. [4].

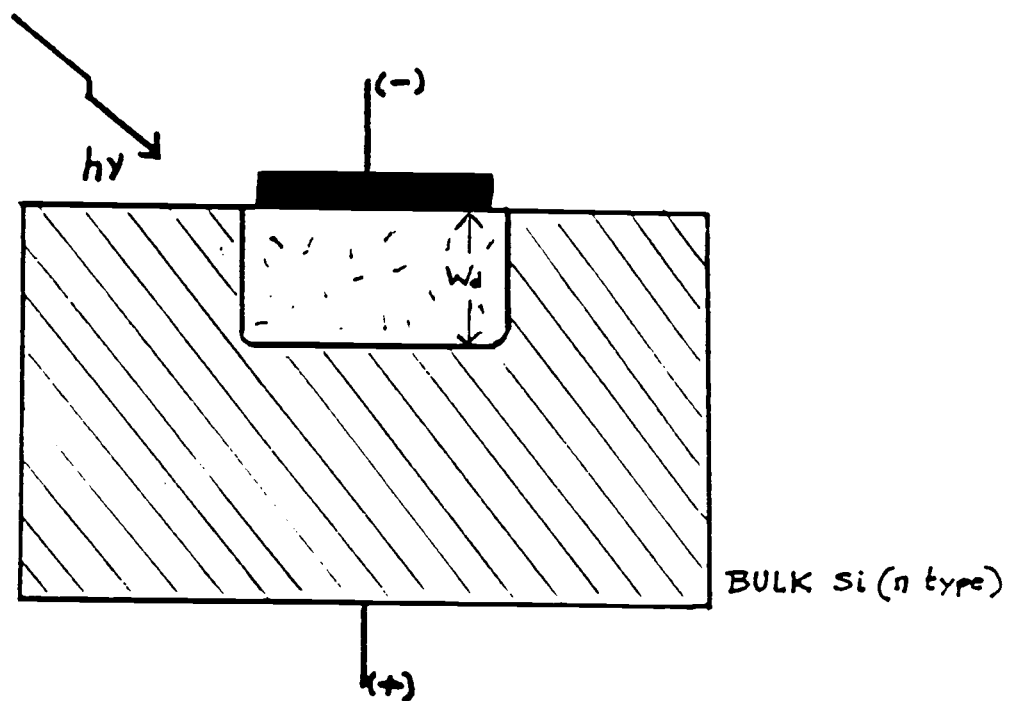


Figure 4) Cross-sectional view of the Schottky diodes used for the experiments.

The change in the depletion width needs to be analyzed under two stipulations:

1. The voltage drop across the junction remains unchanged,
2. The total charge within the semiconductor remains unchanged.

The following equations introduce the rates to optically remove carriers from a defect state:

$$e_n^\bullet = \sigma_n^\bullet S \quad (3)$$

$$e_p^\bullet = \sigma_p^\bullet S \quad (4)$$

where  $e_n^\bullet$  and  $e_p^\bullet$  are the optical electron (and hole) emission rates,  $\sigma_n^\bullet$  and  $\sigma_p^\bullet$  are the electron and hole capture rates respectively, and  $S$  is the optical flux in photons/cm<sup>2</sup> sec. The optical properties of a given defect state are totally defined by  $\sigma_n^\bullet$  and  $\sigma_p^\bullet$ , which, are functions of photon energy. In fact in the n-type material,  $\sigma_n^\bullet(h\nu)$  is the optical absorption spectrum of the defect, and  $\sigma_p^\bullet(h\nu)$  is equivalent to the luminescence spectrum. In the p-type material the roles of  $\sigma_n^\bullet$  and  $\sigma_p^\bullet$  are reversed.

The goal of the experiment that constitutes this thesis is to obtain the  $\sigma_n^\bullet(h\nu)$  profile, and understand the implications as applied to the defects being studied.

The rate equations governing the occupation of a defect state of total concentration  $N_T$  are:

$$\frac{dN}{dt} = \left\{ \frac{(c_n + e_p + e_p^\bullet)(N_T - N)}{(c_p + e_n + e_n^\bullet) N} \right\}$$

Let  $a = e_n + e_p + e_p^\bullet$  and  $b = e_p + e_n + e_n^\bullet$  (5)

The solution for this rate equation assuming the trap to be initially empty would then be:

$$N_t = \begin{cases} 0 & t \leq 0; \\ \frac{a}{a+b} N_T [1 - e^{-(a+b)t}] & t > 0. \end{cases} \quad (6)$$

The time constant for this exponential is the sum of all the rates of carrier capture and emission for the defect.

For Photocapacitance transients the optical rates and dominate the kinetics. The measurement technique used ensures that. ( For an n-type material, under the assumption that we are measuring the majority traps corresponding to that defect ). Hence, the time constant is given by:

$$\begin{aligned} \tau &= \frac{1}{a+b} = \frac{1}{(c_n + e_p + e_p^\bullet) + (e_p + e_n + e_n^\bullet)} \\ &= \frac{1}{e_n^\bullet} \end{aligned} \quad (7)$$

on substitution,

$$\sigma_n^{\bullet} = \frac{1}{s\tau} = \sigma_n^{\bullet}(h\nu) = \frac{1}{\tau(h\nu)S(\nu)} \quad (8)$$

The diode if successively irradiated at different wavelengths can thus generate an Optical capture cross - section - wavelength dependence function.

Measurement of capture cross sections for transitions between deep levels and either CB, ( $\sigma_n^{\bullet}$ ) or VB ( $\sigma_p^{\bullet}$ ), is of prime importance since they provide information about ionization energies, phonon coupling, temperature shift, and can constitute a very good test for theoretical calculations.

### III. FABRICATION AND CHARACTERIZATION OF THE SCHOTTKY DIODES

Czochralski-grown ( CZ ) crystals contain oxygen concentrations of about  $1.0 \times 10^{18}/\text{cm}^3$ . These oxygen atoms are interstitial, and are electrically inactive. During subsequent crystal growth or thermal gettering cycles, these precipitates act as nuclei of secondary defects such as stacking faults (Fig. 5). It has been proven conclusively that these stacking faults are electrically active.

Wafers for this experiment were provided by two different vendors. These were phosphorous doped, n-type, 100 mm. diameter CZ silicon, of  $\langle 100 \rangle$  orientation with a resistivity of 5-7  $\Omega$  cm. Initial oxygen concentrations varied from 35 ppma to 27 ppma while carbon concentrations were below detectable limits using Nicolet FTIR. (These figures are based on the 1979 ASTM standards). These were then annealed at 750 C for 16 hours in ambient nitrogen (for the nucleation process), followed by an oxidation at 1050 C. (dry, 1 hour) and another anneal at 1050 C (in  $\text{N}_2$  for an hour). The oxidation and annealing at 1050 C. contributes to the growth process for the defects (Fig. 6).

This was followed by a plasma etch (rate of one micron per min.) and a planar etch (rate of five microns per min.). Aluminium was then deposited on the silicon wafer to form Schottky diodes. The aluminium was evaporated through a metal mask to a 5000 A. thickness with an average area of

## STACKING FAULTS GROWTH (BULK)

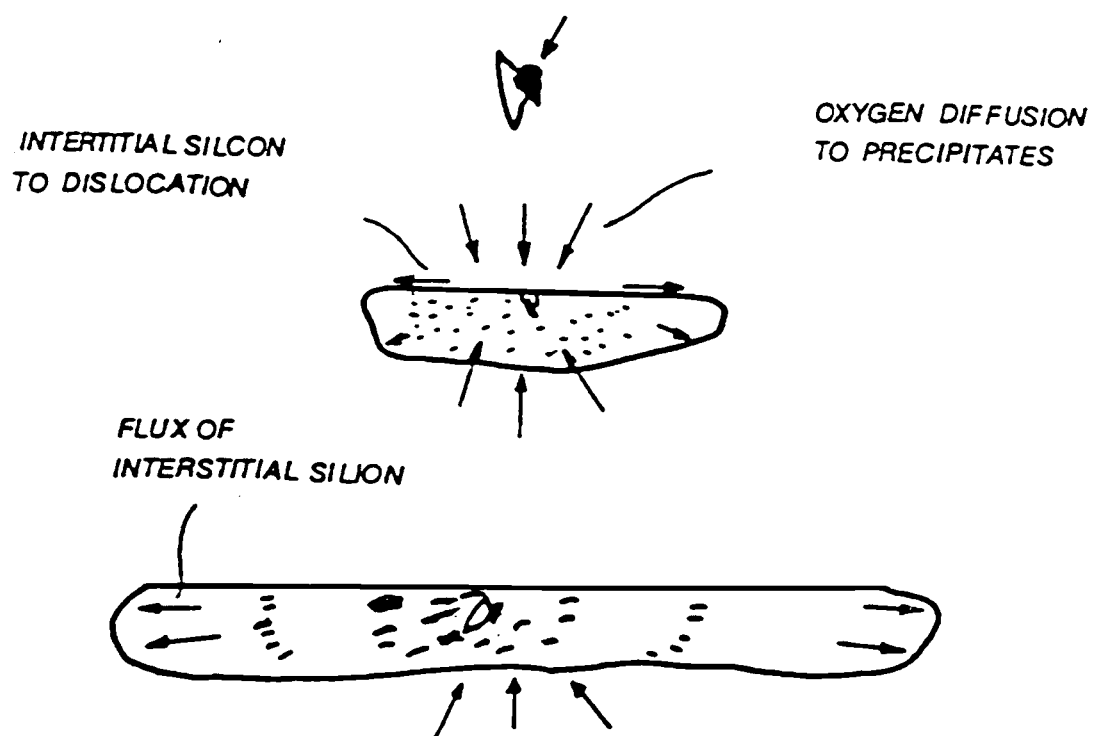


Figure 5) Formation of the Bulk Stacking Faults  
due to interstitial oxygen, after  
L. Forbes et. al. [4]

## TWO STEP HEAT TREATMENTS

### LONG NUCLEATION

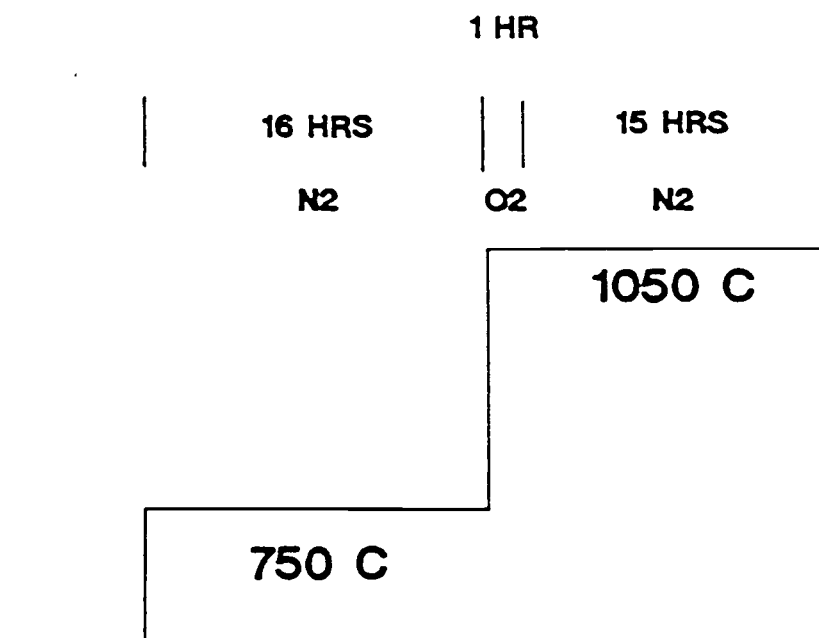


Figure 6) Heat treatments used to generate the Stacking Faults, after L. Forbes et. al. [4].



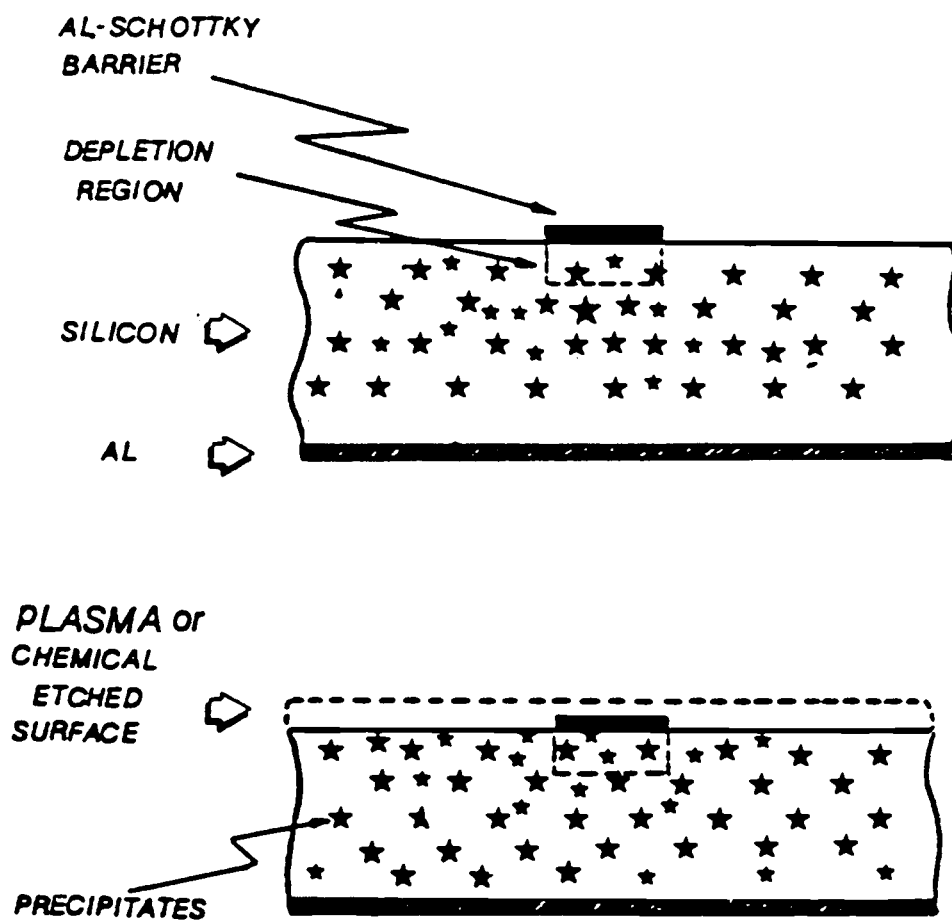


Figure 7) Schematic of the etching done during the fabrication of the Schottky diodes, after L. Forbes et. al [4].

600  $\mu\text{m}^2$  (Fig. 7).

The fabrication of the Schottky diodes was carried out at Hewlett Packard, Corvallis. Each diode was then carefully scribed out from the wafer and mounted on to an IC pad. The diodes were characterized entirely at the Dept. of E&CE at OSU.

The back of the wafer was scribed a little to ensure an ohmic contact, the aluminium was bonded to the positive contact. There is one peculiar factor that one must be aware of while bonding the sample.

Since the diode is to be cooled to a 120 K. during measurement, the epoxy used to bond the wires to the sample must maintain contact at those temperatures. A definitive test for this would be to dip the sample in liquid nitrogen, and check for its characteristics on the curve tracer.

The test diode was then characterized for its current v/s voltage characteristics. Fig. 8. The diode was also tested for its capacitance v/s voltage characteristics (Fig. 9). The diode was then tested for any possible defect states using the DLTS measurement system at the Department of Electrical and Computer Engineering, OSU.

As seen in Fig. 10, sample diodes that showed prominent defect states in the DLTS measurements were selected as candidates for Photocapacitance Transient Spectroscopic analysis.

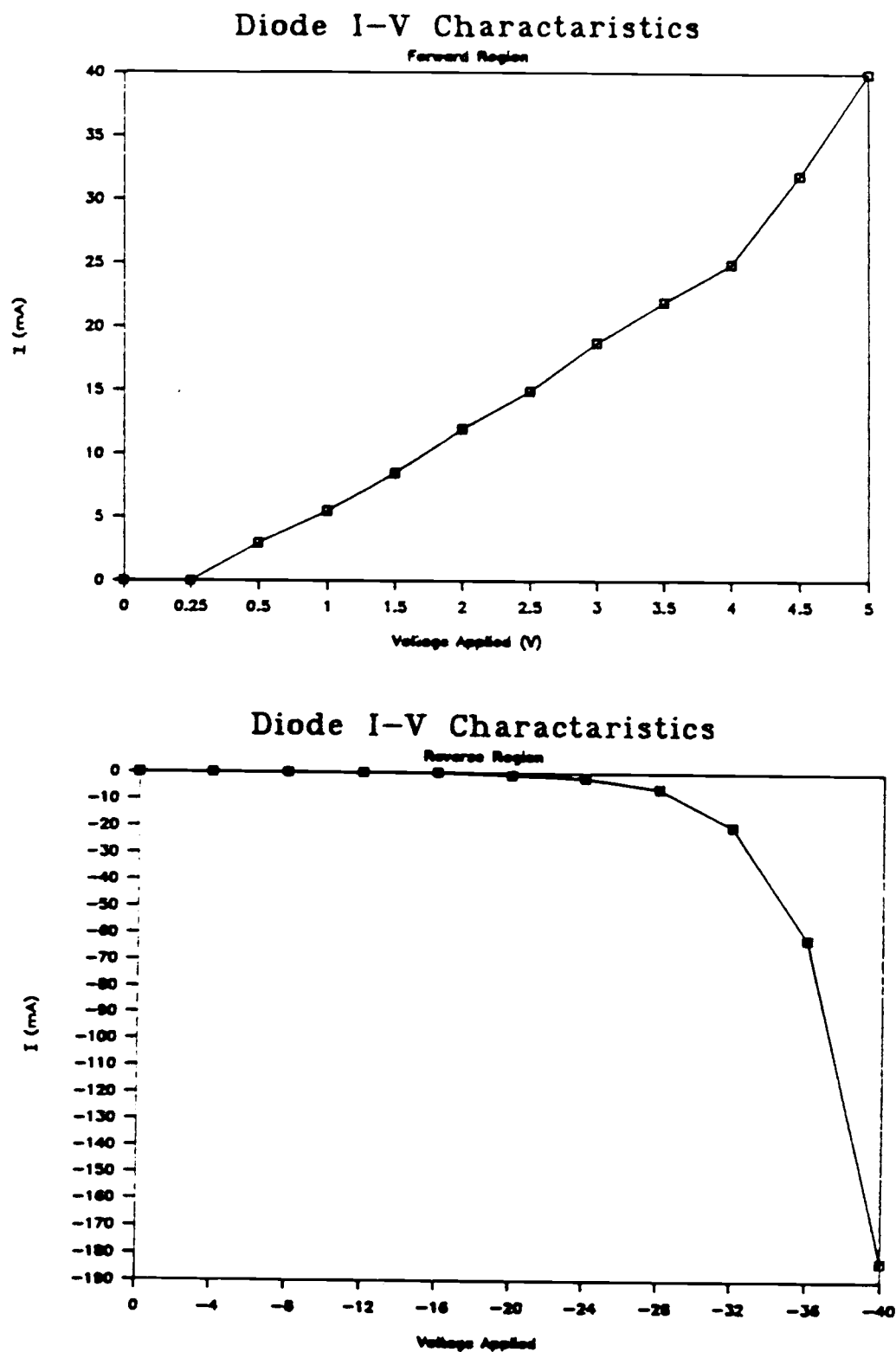


Figure 8) Current v/s Voltage characteristic for a sample diode.

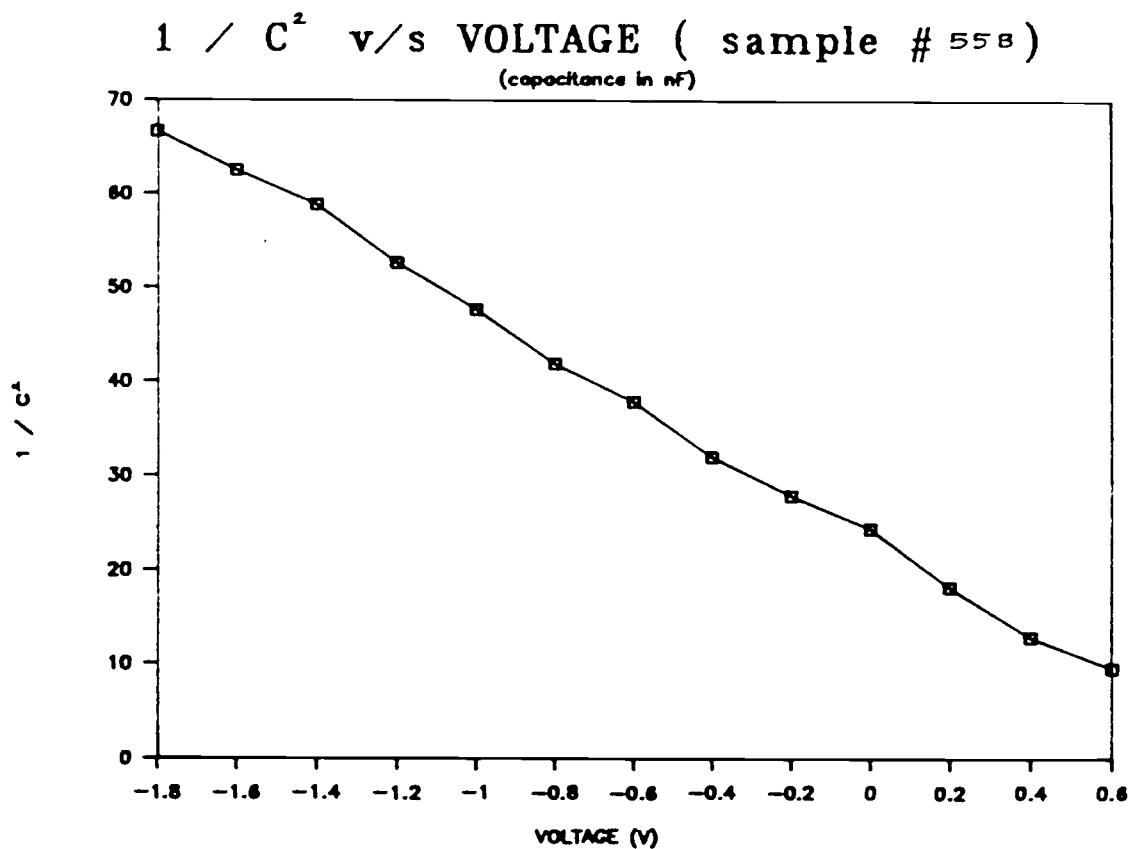


Figure 9) Capacitance v/s Voltage characteristic  
for a sample diode.

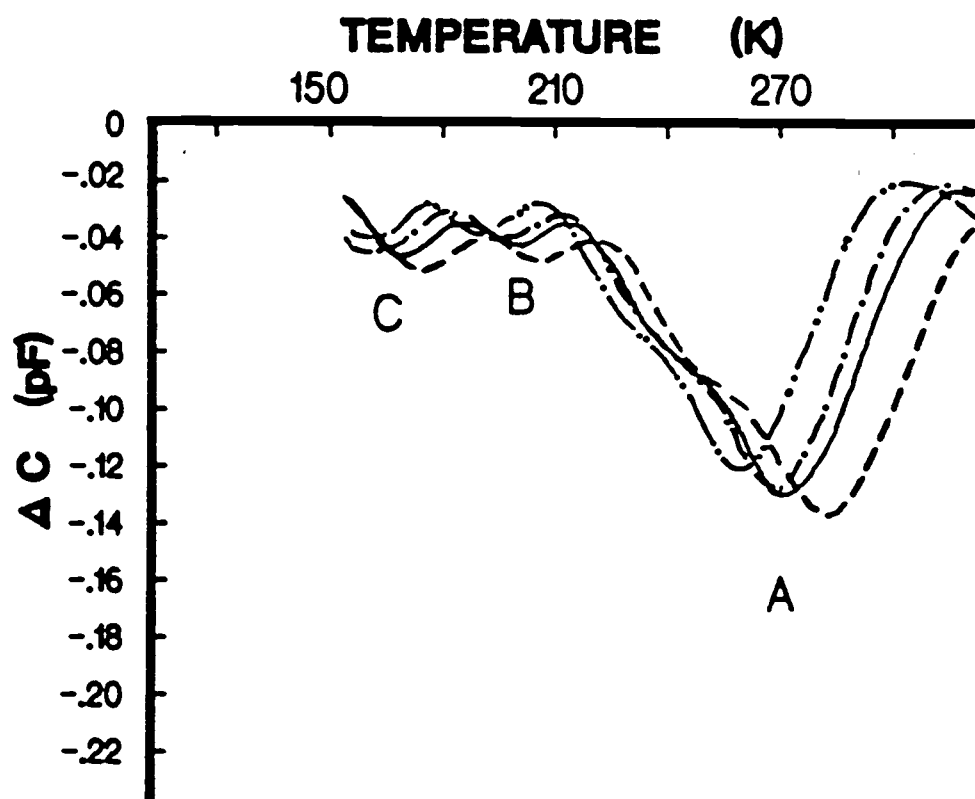


Figure 10) Capacitance DLTS results on a sample diode, after L. Forbes et. al. [4].

#### IV. EXPERIMENTAL SETUP AND PROCEDURE

The experiment is a very sensitive one and demands a well-orchestrated performance from each of its "subsystems". The objective of the measurement dictates the following requirements:

1. An ability to allow a time-controlled exposure to radiation at discrete wavelengths of 100 nm., ranging from 1300 nm., to 3000nm.;
2. An ability to maintain the sample at temperatures as low as 120 K during the measurement;
3. An ability to record the capacitance transient of the optically pulsed Schottky diode;
4. An ability to allow the user to control the sequencing of the procedure involved, to store the data and analyze it.

Each of the requirements above are satisfied by a "subsystem". These are described in detail, followed by a description of the flow of events necessary for a successful measurement.

##### 1. THE OPTICAL SUBSYSTEM:

This subsystem consists of a source of radiation, appropriate filters to cut off the undesirable wavelengths, focussing optics, and a monochromator.

The specific parts used in the implemented setup are:

1. A tungsten light source : variable intensity, voltage controlled.

2. A couple of bi-convex focal lenses (focal length: 10 cm.) and a pair of optical gratings;
3. A Jarrell - Ash monochromator: to select the wavelength of the radiation to be made incident on the Schottky diode;
4. A set of filters: A double sided, polished silicon wafer that cuts off harmonics below 1200 nm., and a germanium wafer that has a cut off at about 2000 nm. ( Fig. 11 ) .

## 2. THE TEMPERATURE CONTROL SUBSYSTEM:

The diode needs to be maintained at a steady 120 K. The diode is mounted on the inner cylindrical support of the "Air-products expander DE-2". It is cooled to a 120 K by an "Air-products HC4 Helium pump". The expander consists of two co-axial hollow cylinders. The diode is mounted on a metal base appended on the inner cylinder. The temperature sensor and the heating element are connected to the metal base. The liquid helium flows in the inner cylinder, axially adjacent to the metal base.

The outer cylinder consists of a metal "sleeve" and a quartz window (transparent at the wavelengths of interest). The diode is maintained at a 120 K. and the quartz window is at room temperature. For the temperature difference to be maintained during the measurement a transparent insulator is essential. A cryogenic pump is used to create the vacuum that prevents the quartz window from fogging up

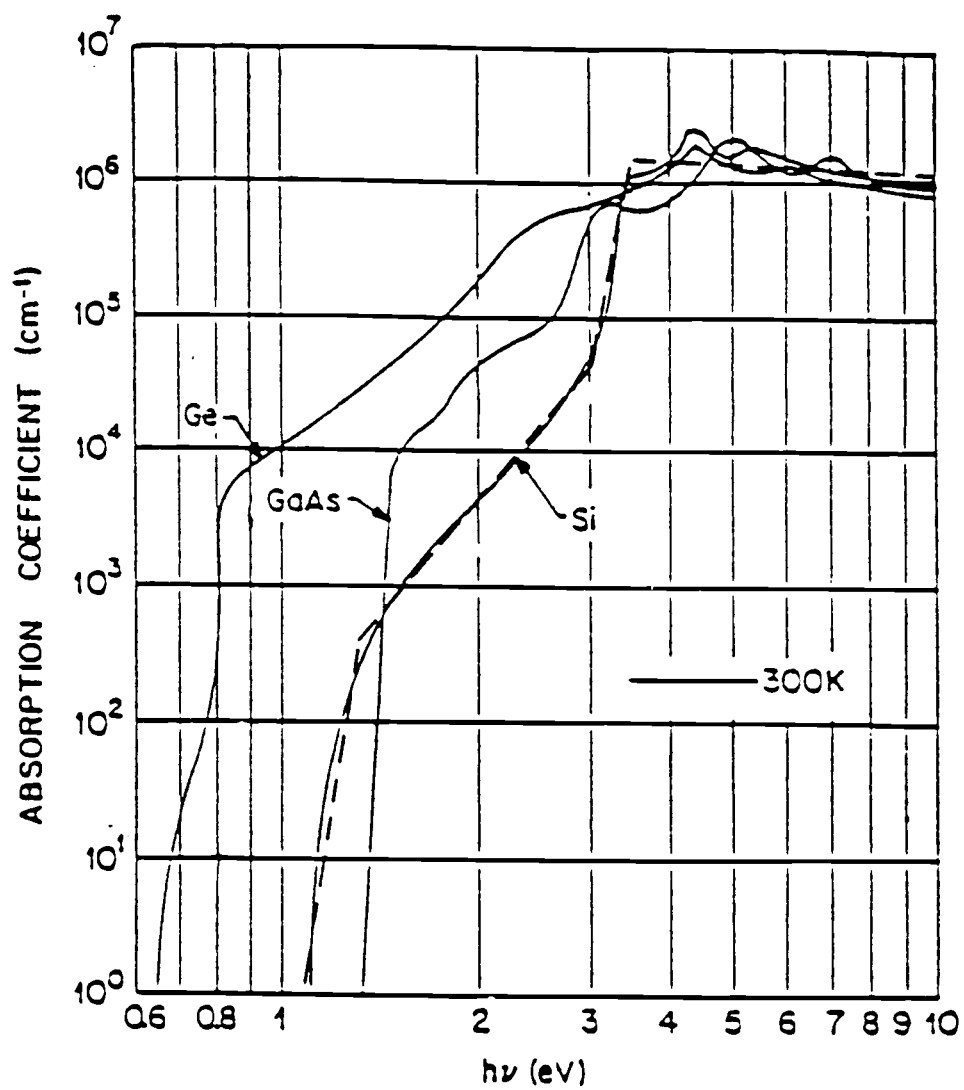


Figure 11) Measured Absorbtion coefficient for  
pure Ge, Si, GaAs, after S.M. Sze, [11].



and allows the diode to be cooled to temperatures as low as 120 K.

The cryogenic pump used works on a simple principle. It contains a metallic container with Xylene in it. A valve connects this container, through a hose, to the expander. Xylene when cooled to low temperatures, sucks in the air between the two co-axial cylinders of the expander. It is cooled in the implemented setup by liquid nitrogen in an ambient container.

A microprocessor controlled temperature sensor (and heating element) is used to maintain the sample at a desired temperature. The liquid helium pump once activated tries to cool the diode down to temperatures as low as 50 K. if left alone. The sensor is pre-set to detect a 120 K. and fire off the heating element at a 120 K. At the desired temperature (in this case, 120 K) the opposing forces of the coolant and the heating element hold the diode in a dynamic temperature equilibrium.

### 3. THE CAPACITANCE TRANSIENT MEASUREMENT SUBSYSTEM:

The Capacitance transient following the optical pulse is recorded on the HP 4280A. The instrument is connected to the diode via two shielded probes, and is connected to the controlling computer via the GPIB bus. This is a very versatile instrument ( can be used for conductance measurements too ) and is capable of sensitivities to 10 fF.

For the parameters that need to be set on the capacitance

meter ( HP 4280 A ), please refer to Appendix B.

#### 4. THE COMPUTER SUBSYSTEM:

The entire experiment is controlled and executed by a program resident in the HP 9000/236 computer. The computer is connected to the HP 4280A (capacitance meter) by the HP-IB bus and has a resident, user-interactive program in its memory that helps the user with the measurement. The program algorithm can be found in Appendix A.

A block - level schematic of the system is shown in Fig. 12. With the subsystems introduced above, a typical measurement would involve the following sequence:

The Schottky diode is tested again for its I-V characteristics using the curve tracer. The characteristics need to be verified for functionality at the low operating temperatures of the system (during measurement).

1. The diode is mounted in the expander, and connected to the HP 4280A via the two shielded probes. The polarity of the mounted diode can be verified by applying a D.C. bias from the HP 4280A and reading the capacitance values displayed. The n-type Schottky diode for example, displays decreasing capacitance values for decreasing bias voltages. If the values appear contradictory to the assumed polarity, the probe connections to the expander (and consequently, the diode) need to be reversed. The outer sleeve of the expander is tacked on, and the diode is ready for alignment to the source of radiation through the optical subsystem.

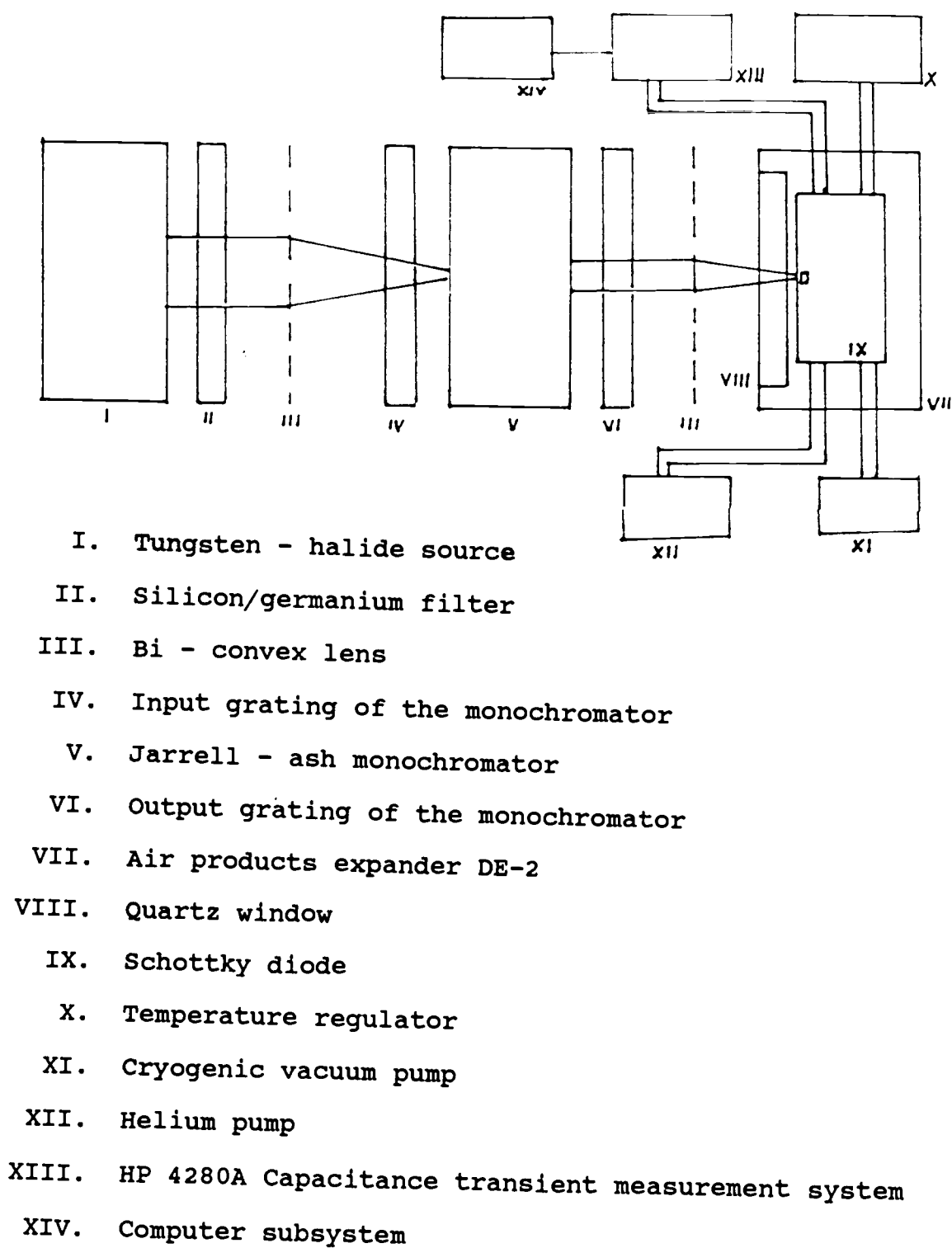


Figure 12) A schematic of the experimental setup.

2. Although the wavelengths used in the measurements lie in the far infrared, for alignment purposes, the monochromator is set to optical wavelengths. The tungsten light source is turned on, and the first bi-convex lens is used to focus the light onto the input grating of the monochromator. The second bi-convex lens (placed between the output grating of the monochromator and the diode) is used to obtain a sharply focused, intense beam to be incident on the diode through the quartz window. The alignment is checked at adjoining wavelengths, and if found to be satisfactory, the lenses are clamped to the surface. This avoids any susceptibility to vibrations that could disturb the focussing and affect the measurement adversely. The diode is now ready to be cooled down to the operating temperature (in this implementation, to a 120 K.).

3. The Xylene container is cooled down to liquid nitrogen temperatures by pouring liquid nitrogen in the encasing container. The valve connecting the container to the expander is opened, and the vacuum almost immediately forces the outer sleeve to be jammed shut. The temperature sensor is set to a 120 K. and the operating mode of the microprocesor control is set to "manual". The liquid helium pump is turned on to initiate the cooling process. The pump itself needs a flow of running water to cool it during its operation: this supply is turned on. The temperature reading needs to be monitored to ensure a smooth cooling down and eventual stabilization. The capacitance reading

during the cooling indicates the nature of the contacts to the expander. If these appear to be abnormal the soldering contacts have been damaged. The sensor is reset to room temperature, the cryogenic pump is turned off, and so is the helium pump. The diode needs to be resoldered to the expander, and the entire process of loading the diode needs to be repeated. If the capacitance during the cooling down appears to be normal( once the diode has been stabilised at a 120 K.) it is ready for the actual measurement.

4. The capacitance transient needs to be obtained at regular intervals of a 100 nm., starting at 1300 nm. The monochromator is set to select the output to be at a 1300nm., the tungsten source is switched on, the diode rechecked for optical alignment if needed, and the silicon filter is inserted in place. A metallic shutter is inserted to block off the radiation from the source to the monochromator. The diode is now in the "dark" state. The program that controls the experiment is then run in the computer, and all the user defined labels are entered on prompts. These include the sample ID, the measurement wavelength, the operating temperature, the number of readings, the d.c. bias to be applied, the interval between each reading, and the number of "beeps" to allow the synchronous release of the shutter. The shutter that has been blocking off the radiation is removed at the last beep. This ensures that the measurement initiation is syn-

chronized to the moment when the diode is exposed to the radiation.

The capacitance meter is now under program control, and this is indicated by the inaccessability of the display to the user. The computer communicates this by displaying the statement "measuring" on the screen and driving the capacitance meter to turn on its L.E.D. implying that measurement is in progress. The completion of the measurement is indicated by the LED on the capacitance meter turning off, and after this, the user is expected to enter "continue" on the computer.

The "continue" enables the capacitance meter to transfer the data to the computer (indicated to the user by the program displaying a message "data transfer" on the screen). At the end of the transfer, the user is asked if he wishes to store the data, if the user wishes to, he is expected to enter the address of the storage space desired; if not, the data is scrolled on the screen.

The program then asks the user if a smooth plot is desired, and the plot generated on the screen. The user may wish to preserve a hard copy of the plot. This can be done most easily by acquiring a screen dump to a printer.

This completes the measurement of the capacitance transient for one wavelength. Since the goal of the experiment is to study the Capture cross section as a function of Wavelength, the same procedure (beginning from the monochromator setting) is repeated for the next wavelength.

At 2000 nm. and higher values of wavelength, the Silicon filter is replaced by a Germanium filter. The time constant for the exponential capacitance rise is then extracted, and translated to the Capture cross section plot, for each of the recorded transients. This generates the capture cross section versus the photon energy profile.

During the measurement, several considerations need careful attention. For precautions that merit attention please refer to Appendix C.

## V. RESULTS AND DISCUSSION

The experiment described in the preceeding section was used to characterize about twenty different samples. The motivation driving these experiments was to observe a correlation between DLTS measurements and Photocapacitance Transient Spectroscopy conducted on the same set of samples.

In terms of prediction of the energy level of the deep donor associated with the defects, DLTS measurements predict a dominant level at  $0.48 \pm 0.05$  eV. below the conduction band. Photocapacitance Transient Spectroscopy predicts a spread of about 0.01 eV. centered around 0.46 eV. below the conduction band.

These predictions are consistent over a range of samples. Capacitance transients are extracted at wavelengths from 1300 nm. to 3000 nm. corresponding to an energy range from 0.4 to 0.9 eV.

The scan covers the range of interest, since DLTS measurements had shown the defects to lie at 0.48 eV. from the conduction band.

A typical Capacitance transient at a wavelength is shown in Fig. 13. An optical pulse stimulates transients from the defect level to the conduction band. This is observed as an exponential variation of the capacitance (associated with the Schottky diode) with time.

A plot of  $\log (\Delta C)$  v/s time is a straight line,



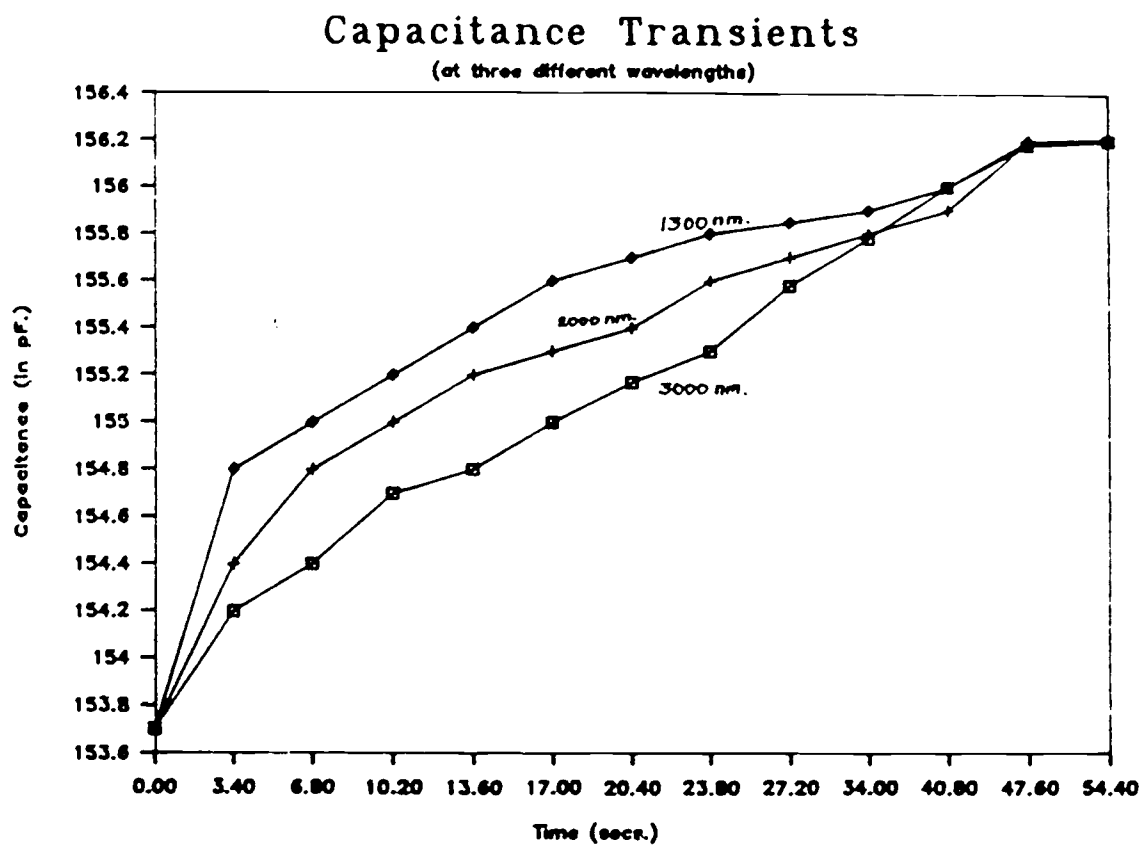


Figure 13) Capacitance v/s Time plot for a sample diode.

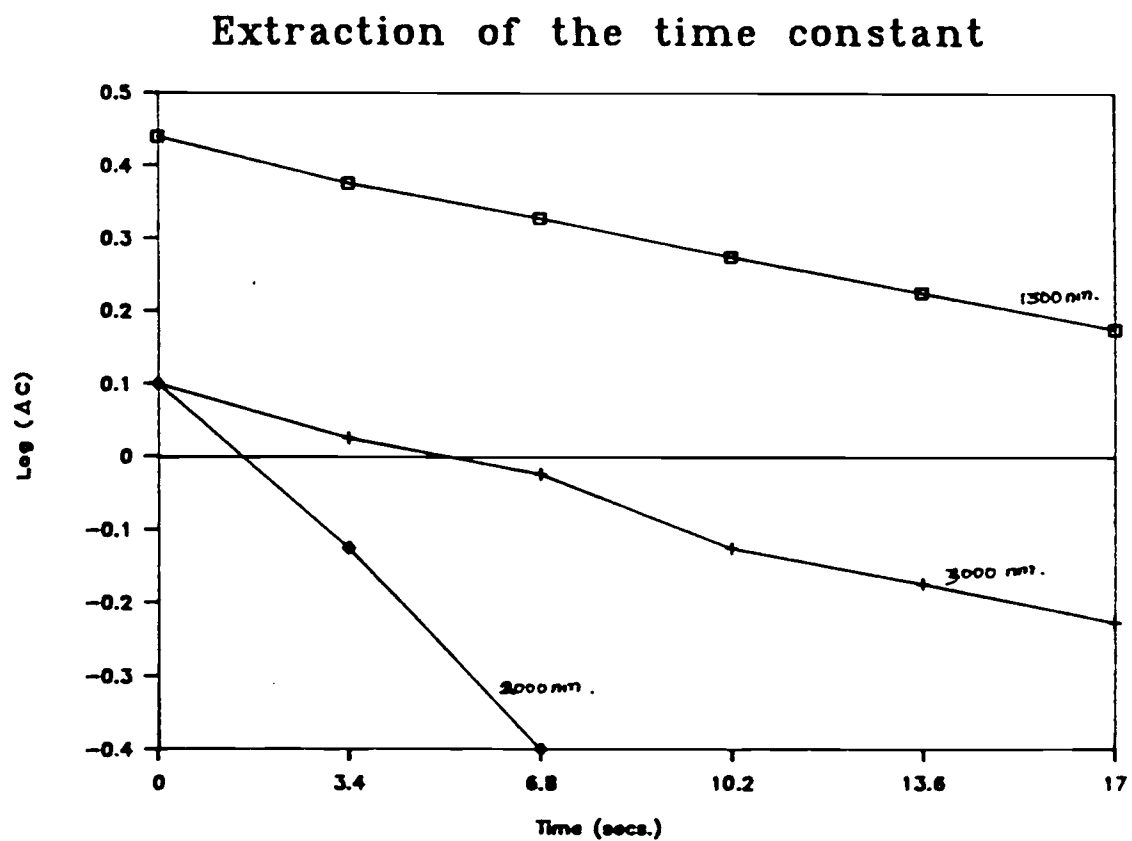


Figure 14) Log ( $\Delta C$ ) v/s time for a sample diode.

confirming the exponential nature of the transition. The inverse of the slope of this line gives us the time constant at the incident wavelength ( Fig. 14 ) .

The Photon flux was measured by a Pyroelectric radiometer. The measured flux times the time constant gives us the inverse of Capture cross section at the incident wavelength.

The incident wavelength was changed from 1300 nm. to 3000 nm. at intervals of a 100 nm. to generate the Optical capture cross-section variation with Wavelength.

The intersection of the locus with the energy axis denotes the energy level associated with the defects.

The experimental results closely follow the Lucovsky model [5]. The slight "flattening out" of the locus at lower photon energies is thought to be due to a spread of energy levels centered around 0.46 ev. The Lucovsky model is based on the assumption that a single, well defined energy level is being investigated. In reality there could be a spread in energy levels associated with the oxygen induced bulk stacking faults. Such a spread of levels is observed for example, at the Silicon - Silicon dioxide interfaces ( Fig. 15 ) .

Since it was impossible to find a single filter that would filter out the harmonics for a range of 1300 nm. to 3000 nm.; a doubly polished piece of silicon wafer was used at the tungsten-halide source from 1300 nm. to 2000 nm., and a piece of germanium wafer was used from 2000 nm. to

3000 nm.

As expected each filter has its own coefficient of absorbtion.

Schottky diodes fabricated from wafers that weren't subjected to the heat cycles (and consequently, had no oxygen induced stacking faults) did not show any capacitive transients in the range of interest.

#### CONCLUSION:

Photocapacitance Transient Spectroscopy is proved to be an effective technique in analyzing deep donors in Silicon. It is a very sensitive technique and could also be used to analyze defect states in other semiconductors.

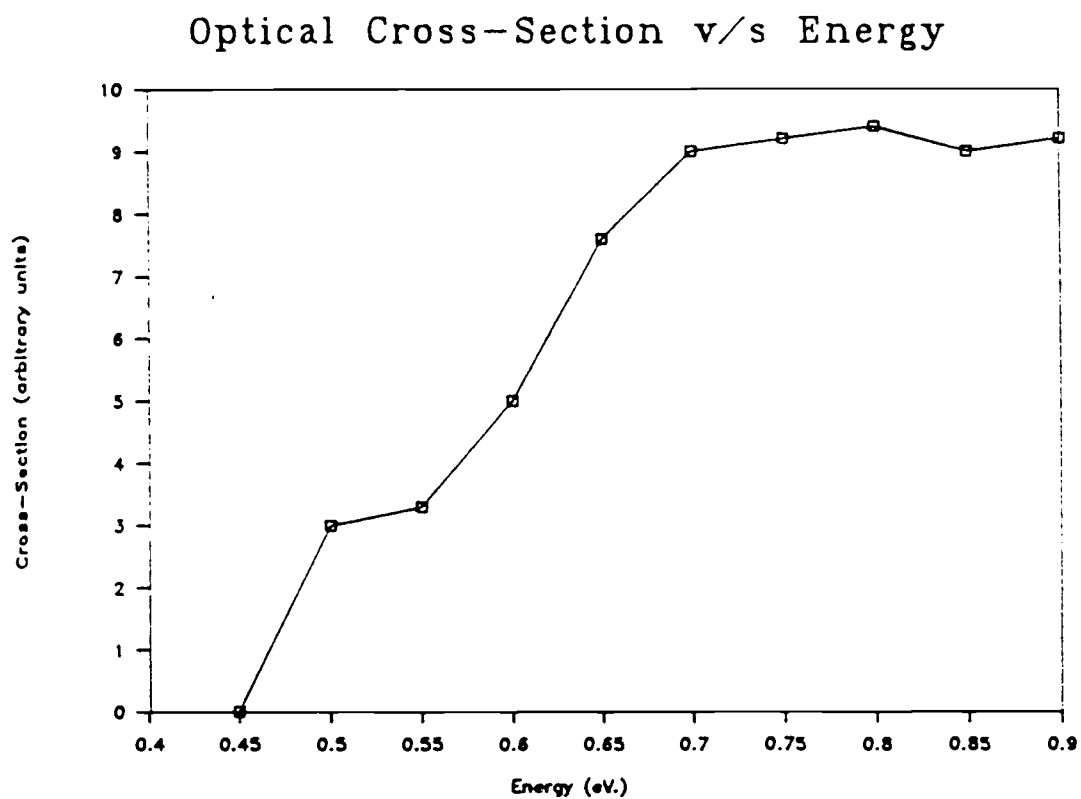


Figure 15) Optical Crosssection dependance on photon energy for a sample diode.

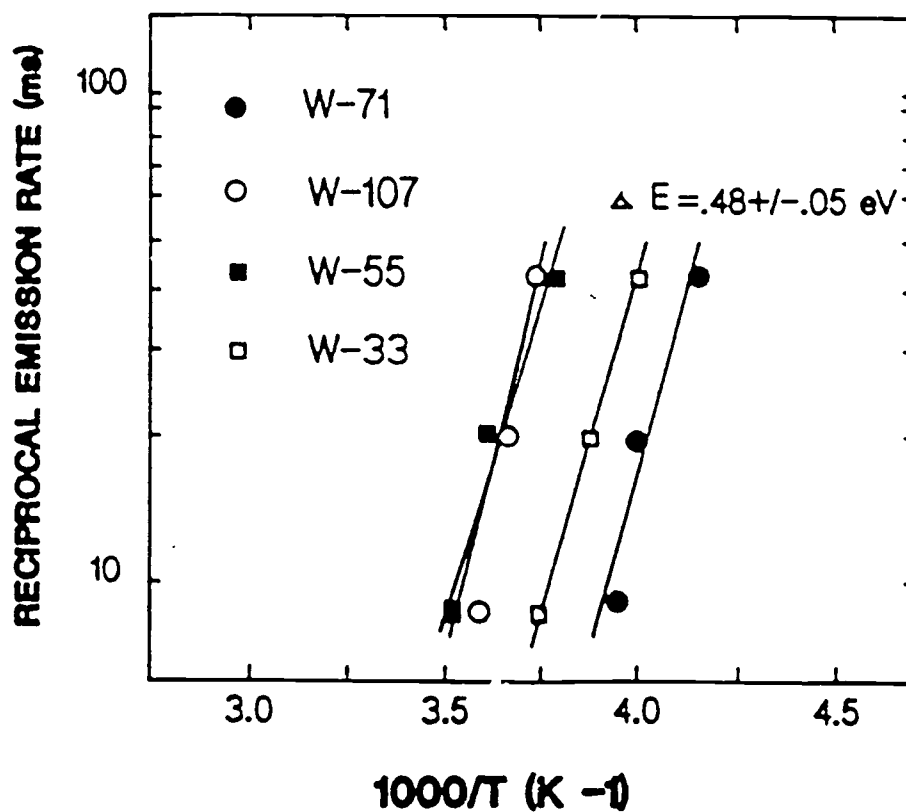
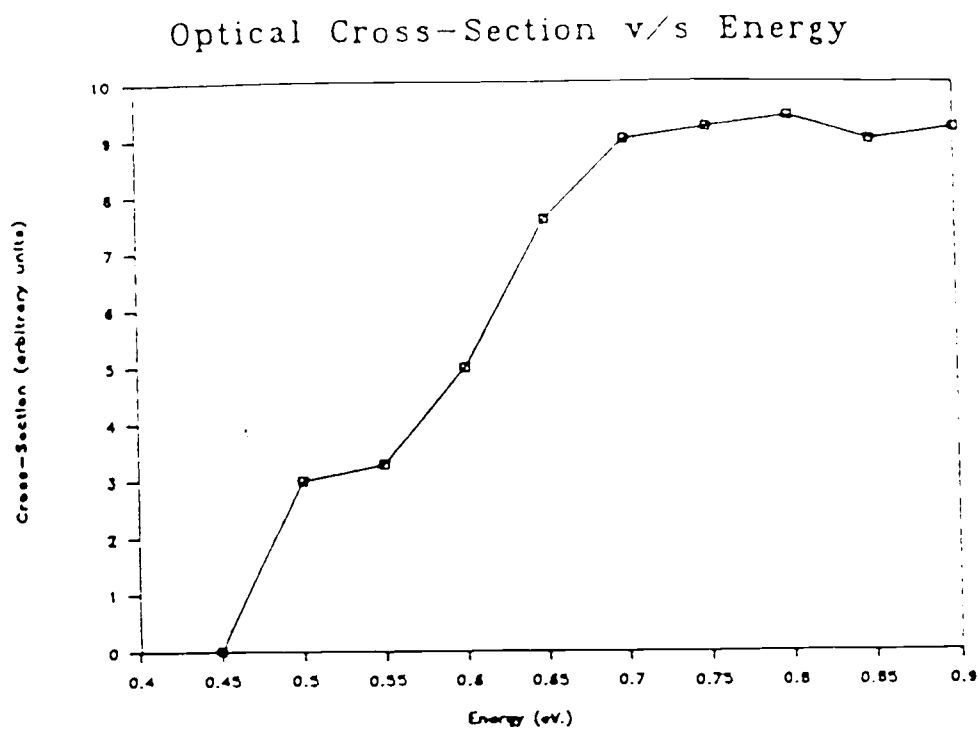


Figure 16) A comparison between DLTS and PCTS  
for sample # 55B

## VI. REFERENCES

- [1] C.T. Sah, L. Forbes, L.L. Rosier, A.F. Tasch, Jr., "Thermal and Optical Emission and Capture rates and Cross sections of electrons and holes at Imperfection centers in Semiconductors from Photo and dark Junction current and Capacitance experiments", Solid State Electronics, Vol. 13, pp. 759-788, 1970.
- [2] A.M. White in: Physics of Semiconductors 1978 (Inst. Phys. Conf. Ser. No. 43, 1979) pp. 123-132.
- [3] D. Bois, A. Chantre, G. Vincent and A. Nouillahat in: Physics of Semiconductors 1978 (Inst. Phys. Conf. Ser. No. 43, 1979), pp. 295-298.
- [4] L. Forbes, H. Haddad, "Electrical Activity of Bulk Stacking Faults in Silicon", Vol. 7, No. 3, Materials Letters, Sept. 1988, pp. 99-101.
- [5] G. Lucovsky, "On the Photoionisation of Deep Impurity Centers in Semiconductors", Solid State Communications, Vol. 3, pp. 299-302, 1965.
- [6] G.L. Miller, D.V. Lang, and L.C. Kimmerling, in Ann. Rev. Mater Sci. 7, pp. 377, 1977.
- [7] H.G. Grimmeis, in Ann. Rev. Mater. Sci. 7, pp. 341, 1977.
- [8] L.C. Kimerling in: Physics of Semiconductors 1978 (Inst. Phys. Conf. Ser. no. 43, 1979 ) pp. 113-122.
- [9] D.V. Lang in: Topics in Applied Physics, Vol. 37, Springer-Verlag, Berlin 1979, pp. 93-133.
- [10] J.W. Chen, and A.G. Milnes, Ann. Rev. Mater. Sci. 10, pp. 157, 1980.
- [11] S.M. Sze, "Physics of Semiconductor devices", (J. Wiley & Sons Inc., 2 Ed., 1981).
- [12] A.G. Milnes, "Deep Impurities in Silicon", (Wiley-Interscience Publication, 1973).
- [13] L.C Kimerling et. al., Appl. Phy. Lett., Vol. 30, No. 5, March, 1977.
- [14] C. Weigel et. al., Phys. Status. Solidi B 71, 701, 1975.
- [15] R. Pierret et. al., "Modular Series on Solid State Devices" Vol. 6, (Addison-Wesley, 1987) pp. 147.

## APPENDICES



## APPENDIX A

## MEASUREMENT ALGORITHM

1. Ask for ID#, Wavelength ( in nm. ) and temperature(in K), store the values typed in by the user;
2. Initialize the HP 4280A as per the requirements of the C-t measurements, tell the user that the HP 4280A is now under program control ( lock out the display );
3. Ask the user for the no. of readings (  $\leq 680$  ), d.c. bias that needs to be applied to the diode ( in V. ), measurement interval between readings (in sec. ), and store the responses;
4. Ask the user for the delay time needed for the synchronization of the shutter release, store the number of "beeps" desired, start the beeps;
5. At the end of the count commence measuring the capacitance transient, tell the user that the HP 4280A is currently in the measurement mode ( display "measuring...." );
6. At the end of the measurement the user is prompted to enter "continue" by shutting off the measurement indicating LED on the 4280A, upon the user entering "continue", transfer the data from the HP 4280A to the computer;
7. At the end of the transfer, ask the user if he wishes to store the data, if yes, wait for the user specifica-

tion of the drive he wishes to store the data in, else, display it on the screen;

8. Ask the user if a smooth/unsmooth plot desired. Upon user prompt select the corresponding subroutine;
9. Plot the data on the screen in graphic form;
10. The user may wish to get a hard copy of the plot. Upon a "dump screen", print the data on the line printer.

This completes the measurement algorithm. As is evident, it is highly user-interactive. The process could be fully automated with default time-outs after every option, but the user needs to retain control of the program, since he may need to start once over at any stage. The analysis, plotting and printing of the data are fully automated.

## APPENDIX B

## PARAMETRIC SETTINGS ON THE HP 4280A

For the measurement of the capacitance transient certain parameters need to be set on the Capacitance meter. These are included here for the sake of completeness of this report. These can be set by executing the resident program in the computer that controls the experiment.

1. "BC": Buffer clear
2. "TR3": Trigger hold
3. "FN5": C-t measurement mode
4. "SL2": Signal level 30 Volts (RMS)
5. "CN10": Floating Mode
6. "IBO": Internal Bias ON
7. "RM3": 1 nF/ 10 ms. range
8. "MS2": Fast measurement speed
9. "LE3": Cable Length 0-5 m.
10. "MAO": Math OFF
11. "BL1": Block Data Transfer Mode
12. "MD1": Data Ready - Mask off
13. "SAO": Burst Integration Mode

The parametric settings above can be easily modified if needed, by changing them as basic statements in the resident program.

## APPENDIX C

### PRECAUTIONS TO BE TAKEN DURING THE MEASUREMENT

During the measurement, the following considerations need careful attention:

1. The silicon and germanium wafers used as filters (to filter out the higher harmonics) absorb the source radiation, and reflect a part of it. These need to be polished to obtain a mirror like surface to minimize surface scattering. Thin wafers need to be chosen to minimize the absorption by the filters.
2. The diode is bonded to the IC pad using a thin gold wire and epoxy glue. The epoxy needs to be chosen such that it continues to bond the wire to the diode at temperatures as low as 120 K. A practical method to test this is to check for the diode characteristics on a curve tracer. The diode when dipped in liquid nitrogen should continue to show acceptable diode characteristics on the curve tracer. Since liquid nitrogen tests the bonding at 77 K, the bond is guaranteed to be a good one at 120 K.
3. The vacuum created by the cryogenic pump assumes an absolutely air-tight hose connection to the expander. Any minute leak causes the Quartz window to fog over. The condensed water vapour leads to absorption and scattering at the wavelengths of interest, leading to a repetition of

the entire algorithm.

4. The optical system must be mounted to resist any mechanical displacements. The bi-convex lenses used for focussing have been positioned to optimize the incident radiation on the diode. Any movement would lead to a weaker intensity incident on the diode, and consequently, less reliable results.

5. The HP 4280A probes have been shielded to ensure sensitivity to 10 fF values; the setting on the HP 4280A must be chosen to accurately estimated cable lengths used. The probe shields must be physically separated during the measurements.